Electro-catalysts for Hydrogen Production from Ethanol for Use in SOFC Anodes

M.A. da Silva, R. da Paz Fiuza, B.C. Guedes, L.A. Pontes, J.S. Boaventura

This document appeared in

Detlef Stolten, Thomas Grube (Eds.):
18th World Hydrogen Energy Conference 2010 - WHEC 2010
Parallel Sessions Book 1: Fuel Cell Basics / Fuel Infrastructures
Proceedings of the WHEC, May 16.-21. 2010, Essen
Schriften des Forschungszentrums Jülich / Energy & Environment, Vol. 78-1
Institute of Energy Research - Fuel Cells (IEF-3)
Forschungszentrum Jülich GmbH, Zentralbibliothek, Verlag, 2010
ISBN: 978-3-89336-651-4

Electro-catalysts for Hydrogen Production from Ethanol for Use in SOFC Anodes

Marcos Aurélio da Silva, Raigenis da Paz Fiuza, Bruna C. Guedes, Luiz A. Pontes, Jaime Soares Boaventura, Energy and Materials Science Group, GECIM, Institute of Chemistry, Physical Chemistry Department, UFBA, 41170290, Salvador, Bahia, Brazil

Abstract

Nickel and cobalt catalysts, supported on YSZ, were prepared by wet impregnation, with and without citric acid; the metal load was 10 and 35% by weight. The catalyst composition was studied by XRF, XPS, and SEM-EDS. At low metal concentration, the results of these techniques presented comparables figures; at high concentration, SEM-EDS suggested a non-uniform distribution. The analysis showed that the solids were mixed oxides and formed an alloy after reduction. The surface passivation was possible under controlled conditions. The catalytic test with the steam reforming of ethanol indicated that the metal load had almost no effect on the catalytic activity, but decreased its selectivity. Afterwards, a unitary SOFC was prepared with deposition of the cathode layer. AFM and EIS were used for the characterization of SOFC components. They showed that the electro-catalyst surface was almost all covered with the metal phase, including the large pore walls of the anode. The YSZ phase dominates the material conductance of the complete SOFC assembly (anode/electrolyte/cathode). The unitary SOFC was tested with hydrogen, gaseous ethanol or natural gas; the SOFC operating with ethanol and hydrogen fuel presented virtually no over-potential.

Keywords: SOFC, ethanol, AFM, SOFC, EIS, XPS.

1 Introduction

Fuel cells are devices that directly convert the fuel chemical energy into electricity, with high efficiency and low pollutant emission. Among the several models, the solid oxide fuel cell (SOFC) attracts special interest. Because of its high operating temperature (800 – 1,000 °C) the SOFC presents high flexibility in fuel choice and the possibility of direct reform in the anode [1, 2]. The hydrogen production from the steam reforming of ethanol has attracted interest mainly for the use of bio mass in fuel cells [3]. Among transition metals, the high C–C bond-breaking activity and the relatively low cost of Ni and Co make it a suitable active phase for ethanol-reforming reactions [4]. Organic additives, including citric acid, have been added to act as a dispersant for a higher specific surface area of the support and a better distribution of active sites of the metal supported catalyst [5]. Atomic Force Microscopy (AFM) and X-ray photoelectron spectroscopy (XPS) are very well established techniques to probe the surfaces of most catalysts. [6, 7] Electrochemical impedance spectroscopy (EIS) has been extensively used to characterize fuel cells [8]. However, the simultaneous use of these three techniques has been relatively scarce [9]. Anodes prepared with nickel and cobalt supported on YSZ and with high metal load (35%) have been used in the preparation

of the solid oxide fuel cell (SOFC) [10] 4. The use of ethanol in the SOFC showed performance comparable to other fuels such as methane and hydrogen [11] 5.

2 Experimental

The wet impregnation method, with and without citric acid addition, was used for the catalyst syntheses. The support (YSZ), metal precursors (Ni and Co) and citric acid were mechanically mixed, with subsequent addition of small amounts of water for better homogenization of the mixture. The catalysts were calcined at 800 °C for two hours in air. The metallic composition of the catalysts samples were determined by XRF, SEM-EDX and XPS while the structure of the solid phase was analyzed by XRD. The AFM analyses were conduct on a transversal, clean and new surface, on non-contact mode, no prevent tip wear. EIS was made in air at variable temperature, with stainless steel contacts. The catalysts were evaluated in the ethanol steam reforming.

In the XPS experiments, the catalysts were initially calcined at 800 °C for two hours in air; afterwards the catalyst were reduced in situ with a hydrogen mixture of 10% molar in nitrogen, between 30 and 800 °C, with a heating rate of 10 °C per minute. The NiCo/YSZ catalysts were characterized by XRF, XRD, SEM-EDS, and XPS. XRF and XRD allowed to determine the bulk composition of the solids. The catalysts were characterized by SEM-EDS using a Shimdazu SS 550 model, with a 15 keV electron beam. XRD was performed in a Pananalytical X'Pert diffractometer with an Anton Paar cell for in situ treatment. The XRD analysis was in the following conditions: 16 - 90 °C, step of 0.016, 256 sec/step, time for total analysis: 2:30 h. Both catalysts were analyzed after calcination at 800 °C and exposition to air. Then the solid was exposed to a hydrogen flow, 20 ml/min, at ambient temperature, a diffractogram was registered and the temperature was increased to 250, 300, 350, 400, 450, 500 and 600 °C, using a heating rate of 2 °C/min. At each temperature it was given 30 minutes for temperature equilibration, before registration of the diffractogram. Each cycle of analysis was completed in 48 hours. After analysis under hydrogen, the solid was cooled under hydrogen flow to the ambient temperature, purged 30 minutes with N_2 flow and exposed gently to air for 12 hours. The passivation of the solid surface under controlled conditions was studied. XPS analysis was performed to determine the surface composition and the oxidation state of the elements at the surface. The spectra were obtained in an ESCALAB VG MKII using non-monochromatized Mg Kα radiation (1253.6 eV). The peak of C1s at 284.8 eV was used as reference.

3 Results and Discussion

Table 1 shows the catalyst composition measured by several techniques. The solid composition determined by XRF agreed with the nominal composition. The XPS analysis showed that the Ni surface concentration is close to its bulk concentration, but Co surface concentration was higher compared to the bulk concentration. These results agreed with the semi-quantitative XRF results for 5Ni5Co and 5Ni5Co-CA samples observed. The SEM-EDS analysis showed that the surface distribution of Ni and Co is not homogeneous, with regions with higher Ni and Co concentrations. XRD analysis [12] *in situ* showed that the catalyst after calcination formed a mixed oxide (figure 1) and that after reduction a NiCo alloy was formed. After reduction, the solid was carefully placed in contact with air. XRD analysis showed that

the alloy was preserved (figure 2), indicating that the passivation of the solid surface was successful. XPS analyses agreed with these results. The metal bulk was composed of a NiCo alloy; both oxides, Ni_2O_3 and CoO, were present at the surface. Figures 3 and 4 show the XPS spectra of the reduced samples.

Table 1: Compositions of reduced catalyst samples in mass percent, by XRF, SEM-EDS, and XPS.

Sample	XRF		SEM-EDS		XPS	
	Ni	Co	Ni	Co	Ni	Co
5Ni5Co	4.7	4.0	7.6	7.2	5.4	7.4
5Ni5Co-CA	4.9	4.2	6.4	6.0	5.4	7.3
32Ni3Co-CA	29,5	3,9	54.8	6.7	31.3	3.6

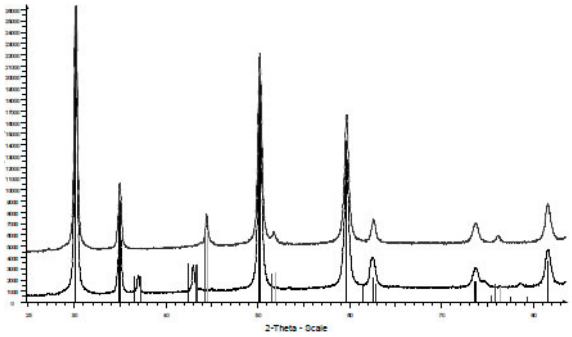

Figure 1: Diffractograms of calcined and reduced samples.

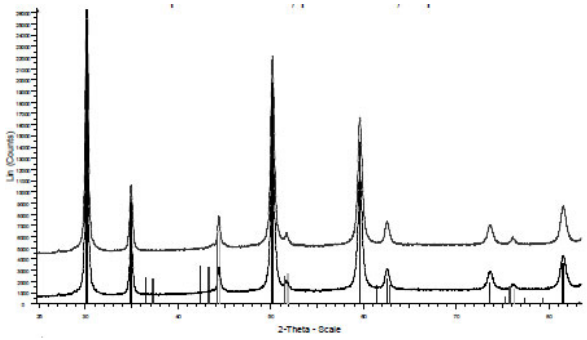

Figure 2: Diffractograms of the passivated sample.

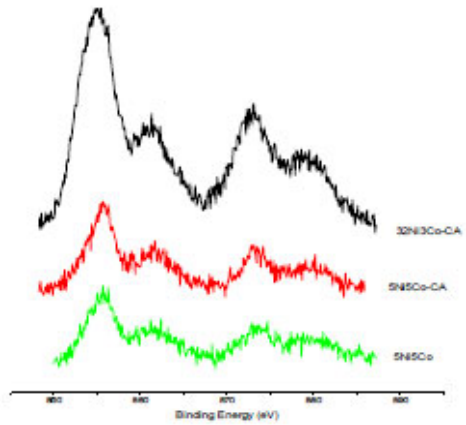

Figure 3: XPS of the calcined and reduced samples.

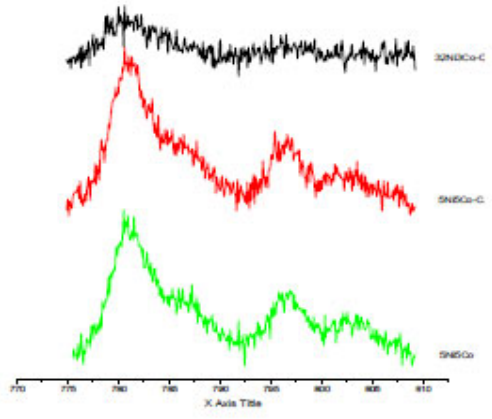

Figure 4: Diffractograms of the passivated sample.

Figure 5 showed the results of catalysts evaluation in ethanol steam reforming. Sample with higher metallic load presented slightly higher conversion of ethanol; they also showed lower selectivity for hydrogen production. Among the sample of low metallic load, the catalyst prepared with citric acid showed high selectivity. These result suggested that citric acid acted as a dispersant of metallic phase.

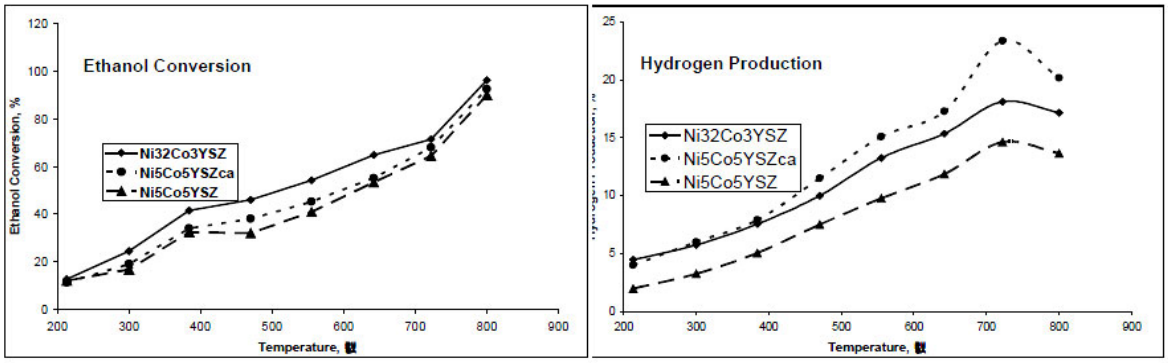

Figure 5: Ethanol conversion and hydrogen production in the ethanol steam reforming.

Figure 6 shows AFM analyses of the surface of the electro-catalyst prepared with YSZ and Ni (no Co was present). Region A (anode), surface had large holes (~1 mm) with depth exceeding 5 mm; probably the holes are vertical, since the images showed a V profile. Region B (electrolyte), the surface presented no holes, with 85 nm roughness on large scale, and 1.7 nm on small scale. Region C (cathode), the surface was very flat, with roughness of 72 nm, on a large scale, and 2 nm on small scale.

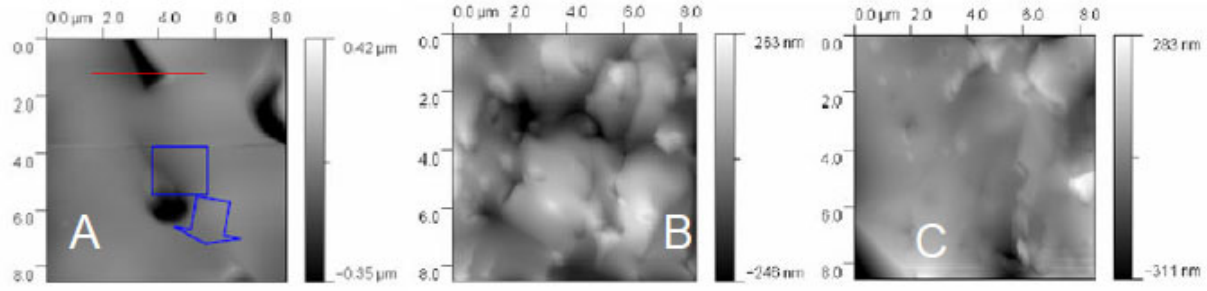

Figure 6: SOFC component AFM: a) anode (Ni/YSZ), b) electrolyte (YSZ), c) cathode (LSZ).

Figure 7 shows that the impedance decreased with increasing temperature, which indicated a raised ionic conduction for high temperatures; the impedance lowered for large frequencies. The impedance module, measure at 700 ºC and 106 Hz, was 5.1, 6.7, and 8.1 x 10^3 for the cathode/electrolyte/anode pellet, anode (Ni/YSZ) and electrolyte (YSZ) layers, respectively. From 700 to 400 ºC, the conductance activation was 0.5, 1.1, and 1.2 eV for the three materials. Apparently, for the anode and electrolyte layers, the YSZ dominated the conduction process. The electro-catalyst surface is almost all covered with the metal, including the large pore walls. The YSZ phase dominates the material conductance of the complete SOFC assembly (anode/electrolyte/cathode).

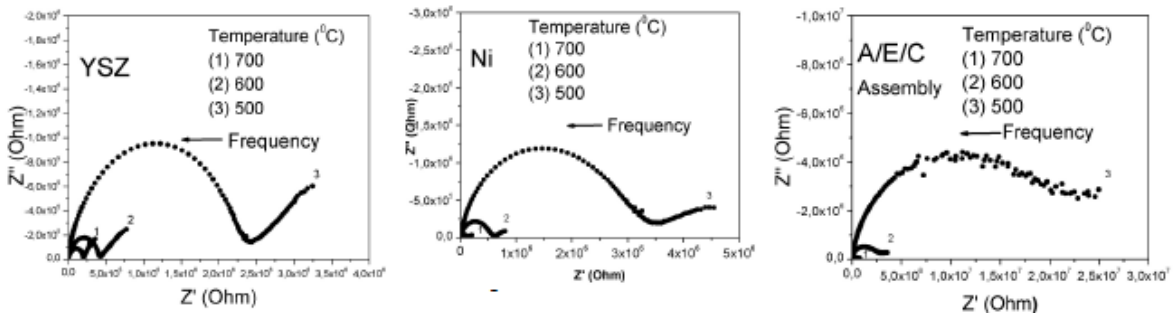

Figure 7: SOFC component EIS: a) anode (Ni/YSZ), b) electrolyte (YSZ), c) cathode (LSZ).

The unitary SOFC has been tested with hydrogen, gaseous ethanol or natural gas. The SOFC performance with the various fuels is shown in figures 8 and 9. One of the most remarkable features of the SOFC operating with ethanol and hydrogen fuel was the virtual absence of overpotential. This cell property is directly related to internal ohmic resistances, the lower the overpotential the lower the internal resistance. Therefore, the very low overpotential presented by the unitary SOFC was likely resulting from the excellent interface formed between the electrolyte and electrodes.

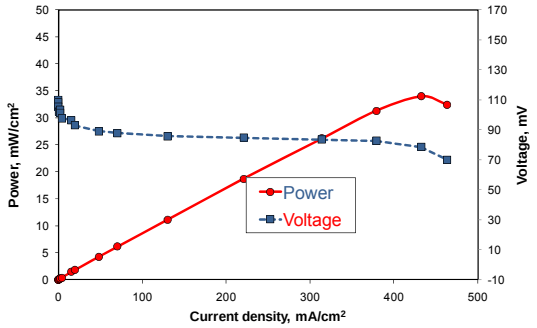

Figure 8: SOFC performance with ethanol at 800 °C (voltage and power density *versus* current density).

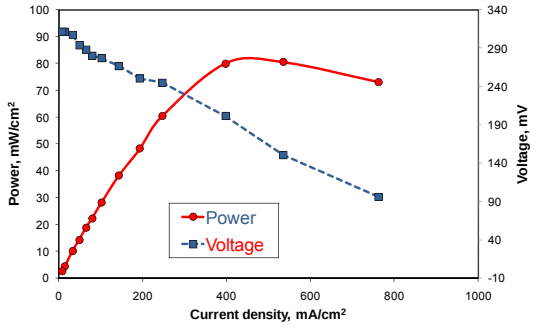

Figure 9: SOFC performance with methane at 800 °C (voltage and power density *versus* current density).

4 Conclusions

The analysis showed that the metal phase of the prepared catalysts was mixed oxides and that an alloy was formed after reduction. The surface passivation was possible under controlled conditions; after passivation the metal bulk remained as an alloy and the surface was a mixture of Ni and Co oxides. The metallic species were the active site for ethanol reforming, which explained the good activity results for these solids.

Furthermore, the metal, at low concentration, was uniformly dispersed on the catalyst support; different behavior was found for catalysts with high metal load. Nickel and cobalt formed stable alloy on YSZ, which after reduction remained as metal, even after exposure to air. The metal load had almost no effect on the catalytic activity, but decreased the

selectivity. At low metal load, the use of citric acid increased the catalytic selectivity, likely due to its dispersant effect.

Finally, AFM and EIS are very useful techniques for the characterization of SOFC components, being almost obligatory for fuel cell development. The electrocatalyst surface is virtually all covered with the metal, including the large pore walls. The YSZ phase dominates the material conductance of the complete SOFC assembly (anode/electrolyte/cathode).

References

[1] M. A. Silva, Jaime S. Boaventura, M. G. Alencar, C. P. Cerqueira, Revista Matéria, 12 (**2007**) 99

[2] S. C. Singhal and K. Kendall, “High-temperature Solid Oxide Fuel Cells: Fundamentals, Design and Applications”, Elsevier Science, UK, **2004**.

[3] T. A. Maia; J. D. A. Bellido; E. M. Assaf; J. M. Assaf, Química Nova, 30 (**2007**) 339.

[4] M. C. Sánchez-Sánchez, R. M. Navarro, J. L. G. Fierro. International Journal of Hydrogen Energy, 32 (**2007**) 1462.

[5] L. Shen, X. Zhang, Y. Li, X. Yang, J. Luo, G. Xu. Nanotechnology, 15 (**2004**) 337.

[6] T. W. Eom, H. K. Yang, K. H. Kim, H. H. Yoon, J. S. Kim, S. J. Park, Ultramicroscopy, 108 (**2008**) 1283.

[7] M. B. Pomfret, J. C. Owrutsky, R. A. Walker, Analytical Chemistry, 79 (**2007**) 2367.

[8] Y.J. Leng, S.H. Chan, K.A. Khor, S. P. Jiang, International Journal of Hydrogen Energy, 29 (**2004**) 1025.

[9] C. Guizard, A. Princivalle, Catalysis Today, 146 (**2009**) 367.

[10] M. A. Silva, M. G. Alencar, R. P. Fiúza, Fiúza, J. S. Boaventura. Revista Matéria, 12 (**2007**) 72.

[11] M. A. Silva, M. G. Alencar, R. P. Fiúza, Fiúza, J. S. Boaventura. Revista Matéria, 12 (**2007**) 99.

[12] K. D. M. Harris, M. Tremayne, Chemistry of Materials, 8 (**1996**) 2554.